

## Permeability of Cork for Water and Ethanol

Ana Luisa Fonseca,<sup>†</sup> Carla Brazinha,<sup>‡</sup> Helena Pereira,<sup>§</sup> Joao G. Crespo,<sup>‡</sup>  
 and Orlando M. N. D. Teodoro<sup>\*,†</sup>

<sup>†</sup>Center for Physics and Technological Research – CEFITEC, Physics Department, Faculty of Sciences and Technology, Universidade Nova de Lisboa, 2829-516 Caparica, Portugal

<sup>‡</sup>REQUIMTE/CQFB, Chemistry Department, Faculty of Sciences and Technology, Universidade Nova de Lisboa, 2829-516 Caparica, Portugal

<sup>§</sup>Centro de Estudos Florestais, Instituto Superior de Agronomia, Universidade Técnica de Lisboa, 1349-017 Lisboa, Portugal

**ABSTRACT:** Transport properties of natural (noncompressed) cork were evaluated for water and ethanol in both vapor and liquid phases. The permeability for these permeants has been measured, as well as the sorption and diffusion coefficients. This paper focuses on the differences between the transport of gases' relevant vapors and their liquids (water and ethanol) through cork. A transport mechanism of vapors and liquids is proposed. Experimental evidence shows that both vapors and liquids permeate not only through the small channels across the cells (plasmodesmata), as in the permeation of gases, but also through the walls of cork cells by sorption and diffusion as in dense membranes. The present study also shows that cork permeability for gases was irreversibly and drastically decreased after cork samples were exposed to ethanol or water in liquid phase.

**KEYWORDS:** cork, water transport, sealing properties, permeability, sorption, diffusion

### ■ INTRODUCTION

Cork is a natural material having particular characteristics that are at the origin of remarkable applications.<sup>1,2</sup> Cork is known worldwide for wine sealing because it is nontoxic, has good “impermeability” to liquids and gases, lasts several years without apparent loss of sealing performance, and has the ability for compression and stress recovery. Other cork applications, such as an insulator or energy absorber, also rely on particular combinations of these properties.

The chemical and structural compositions of cork are already well-known.<sup>1–5</sup> Cork is a homogeneous cellular material of small and thin-walled cells that are regularly arranged without intercellular spaces.<sup>6</sup> The main structural component of cork cell walls is suberin, representing about 40% of its composition. This hydrophobic lipid is responsible for many of the key cork properties, namely, its tightness to wine. Cork contains also lignin (>20%) and polysaccharides (20%), as well as extractives (15%).<sup>7</sup>

Cork cells do not have intercellular openings or communication structures at the micrometer level such as those present, for example, in wood cells. However, there are very small channels (plasmodesmata) between cells, across the suberized cell wall with a diameter of about 100 nm.<sup>8</sup> These channels play a key role in the transport of gases through cork, as we suggested in previous works by Faria et al.<sup>9</sup> and by Brazinha and coauthors.<sup>10</sup> These channels seem to be the main routes for oxygen ingress in bottled wine with cork closures.

In another work, we also showed that air inside a cork closure is a limited source of oxygen after compression. Only under special bottling procedures and during very few weeks after bottling was some air ingress observed.<sup>11</sup>

However, the transport of condensable vapors and their liquids remains to be described. In particular, the transport of water and ethanol is relevant because cork is frequently exposed

to these species, not only in wine bottling but also in other applications.

There are very scarce data concerning the interaction of cork with vapors and liquids other than water. The literature comprises studies regarding the sorption of heavy metals from contaminated water,<sup>12–14</sup> the sorption and diffusion of phenolic compounds,<sup>15</sup> and the sorption of 2,4,6-trichloroanisole (TCA).<sup>16,17</sup> In these works, cork is referred to as a noninert material interacting with the permeating species. On the contrary, ethanol sorption was reported to cause swelling of cork and to change the SO<sub>2</sub> sorption properties of the material.<sup>18</sup>

Water sorption and diffusion in cork are described in refs 19–23. Rosa et al.<sup>19</sup> obtained diffusion coefficients of liquid water at 20 and 90 °C along directions parallel and perpendicular to the radial direction of boiled cork by immersion in liquid water and by inserting electrodes in cork and measuring electrical resistance between them. Adão et al.<sup>20</sup> also obtained diffusion coefficients of vapor water in boiled cork at 25 °C by exposure to water vapor in a saturated atmosphere. Water sorption was studied by monitoring the changes of mass,<sup>19,20</sup> volume, and linear dimensions of cork in which water caused the expansion (swelling) of cork.<sup>19</sup>

A study of water vapor sorption on crude cork for different sample geometry, for different temperatures, and in a large range of relative pressure was also performed in ref 21. Water sorption was reported to cause swelling of cork, as for wood, due to the cellulose content. A sorption mechanism of water on cork was proposed. First, water sorbs on hydrophilic sites

**Received:** April 10, 2013

**Revised:** September 3, 2013

**Accepted:** September 3, 2013

**Published:** September 3, 2013

constituted by hydroxyl and methoxyl groups through hydrogen bonds, and then sorption continues by water cluster formation around the hydrophilic sites.

None of the reported works focused the differences among gases, which were previously studied in<sup>9,10</sup> liquids and their vapors. Therefore, in the present work we stress this comparison showing the permeation results for gases, vapors, and liquids (water and ethanol) in the same cork sample under well-defined conditions and propose a transport mechanism of vapors and liquids through cork, namely, water and ethanol. Moreover, because these species are the major wine components, our results may be of interest with regard to the recommended position for bottle storage; in a vertical position, cork is exposed to vapors, whereas in a horizontal position, it is exposed to liquid.

Enologists recommend bottles to be placed horizontally for long-term storage of wine. Bottles placed vertically lead to more oxidation,<sup>24</sup> consequently ruining the wine. On the contrary, when bottles are placed horizontally, cork remains moist and swelled, reducing the exposure of wine to air. However, Lopes et al.<sup>25</sup> showed that the storage position had little effect on the oxygen transfer rates for most of the sealing systems tested. Skouroumounis et al.<sup>26</sup> also verified that bottle orientation during storage had only a small effect on composition and sensory properties of the wines examined. The study performed in this work will contribute to clarify this not consensual issue.

## EXPERIMENTAL PROCEDURES

**Sampling.** Samples used to measure the cork permeability were taken from planks of reproduction cork with a 9 year production cycle having a thickness of about 38 mm. These planks underwent the standard boiling procedure as used by stopper manufacturers.<sup>3</sup> Samples were selected and prepared as described in ref 9. Samples had a final shape of small disks, of 10 mm diameter and 2 mm thickness; the tested area was 9.6 mm<sup>2</sup>, corresponding to a 3.5 mm exposed diameter. The cited work<sup>9</sup> provided a picture of the permeability distribution in random samples. Therefore, in this work we chose to use samples with helium permeabilities ranging from  $6 \times 10^{-13}$  to  $6 \times 10^{-12}$  mol/(Pa·m·s), because it covers an integrated probability of about 80% of the obtained distribution.

For sorption experiments boiled cork of the same type was used after trituration into 1–2 mm particles by using a ball mill (model Mixer Mill MM2, Retsch) to increase the transfer area between cork and the sorbing species.

**Permeability Measurements.** A helium mass spectrometer leak detector (Adixen ASM 142D) was used to directly measure the He permeation. This technique allows a quick measurement of the He flow through a membrane as demonstrated in ref 9. The sample holder was connected directly to the test port of the leak detector. The upstream side was evacuated to pressures down to 1 mbar and then filled with He to a feed pressure  $p_f$  of 1 atm. The pressure in the downstream side  $p_d$  was monitored as a function of time while a constant pressure of the permeant was applied to the upstream compartment. The permeability  $P_e$  (m<sup>2</sup>/s) was calculated from the measured volumetric gas flow rate  $Q$  (Pa·m<sup>3</sup>/s) by taking into account the thickness of the sample  $\delta$  (m), the permeation area  $A$  (m<sup>2</sup>), and the pressure difference of the compound under study  $\Delta p = p_f - p_d$  (Pa) as

$$P_e = \frac{Q\delta}{A\Delta p} \quad (1)$$

In the case of other gases, vapors, and liquids, permeation was measured by the pressure rise method.<sup>27</sup> The volumetric flow rate,  $Q$ , is then given by

$$Q = V \frac{dp_d}{dt} \quad (2)$$

where  $V$  (m<sup>3</sup>) is the downstream volume and  $t$  (s) is the elapsed time. The pressure rise setup is illustrated in Figure 1. After sample

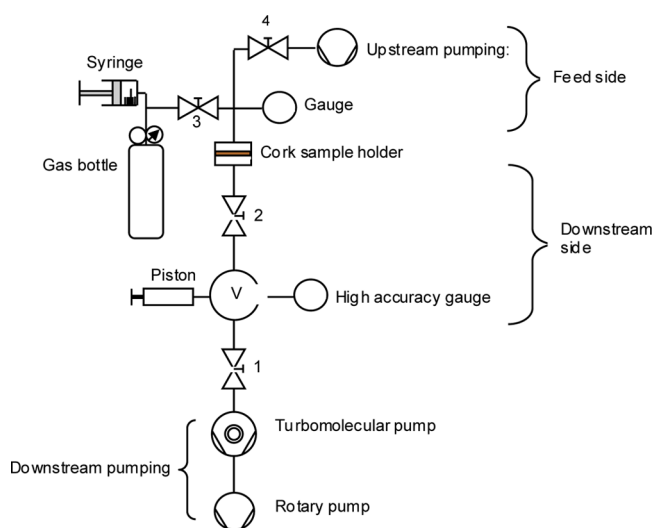


**Figure 1.** Pressure rise experimental setup. The upper side volume was filled with the permeant species (vapor or liquid). The pressure in the downstream volume,  $V$ , was monitored by a high-accuracy gauge.

introduction in the sample holder, the downstream side was evacuated to a pressure below  $10^{-5}$  mbar to ensure proper surface outgassing of this volume. At the same time the upstream side was evacuated to pressures below 0.1 mbar. Then, valve 1 was closed, valve 3 was opened, and the feed side was ready to be filled with the permeant species under study. Vapors and liquids were introduced with the help of a small graduated syringe. In the case of vapors, the feed pressure was well below its vapor pressure to suppress condensation. Both pressures in the feed and the downstream compartments were continuously monitored. The downstream pressure was measured by a high-accuracy gauge (MKS 690A 1 Torr Baratron), for as long as needed to obtain a constant rate. The feed side was connected to an MKS 627B 5 bar Baratron. Both gauges were coupled to a data logger for continuous data acquisition.

A piston was used to measure the downstream volume, needed to calculate  $Q$ . By performing an adiabatic expansion of air having a known  $\Delta V$  and measuring the initial and final pressure, the volume was obtained from Boyle Mariotte's law. The method was repeated for compression, and the average volume was used. The temperature was kept constant and homogeneous by flowing water at controlled temperature in a silicone tube wound around the setup. Two calibrated thermocouples were fitted in different points to monitor the temperature homogeneity.

Table 1 shows the starting feed pressures for the permeability tests in both samples. Tests for liquids were performed by filling the upper side with 5 mL and then leaving the volume open to air. In this case the holder was fitted vertically, to keep the liquid in direct contact with the sample by gravity.

**Table 1.** Starting Conditions for Permeability Tests

	feed pressure (mbar)		saturated vapor pressure at 22 °C (mbar)
	sample A	sample B	
water	17.7	16.6	26.4
ethanol	40.2	35.1	66.5
all other gases	1000	1000	

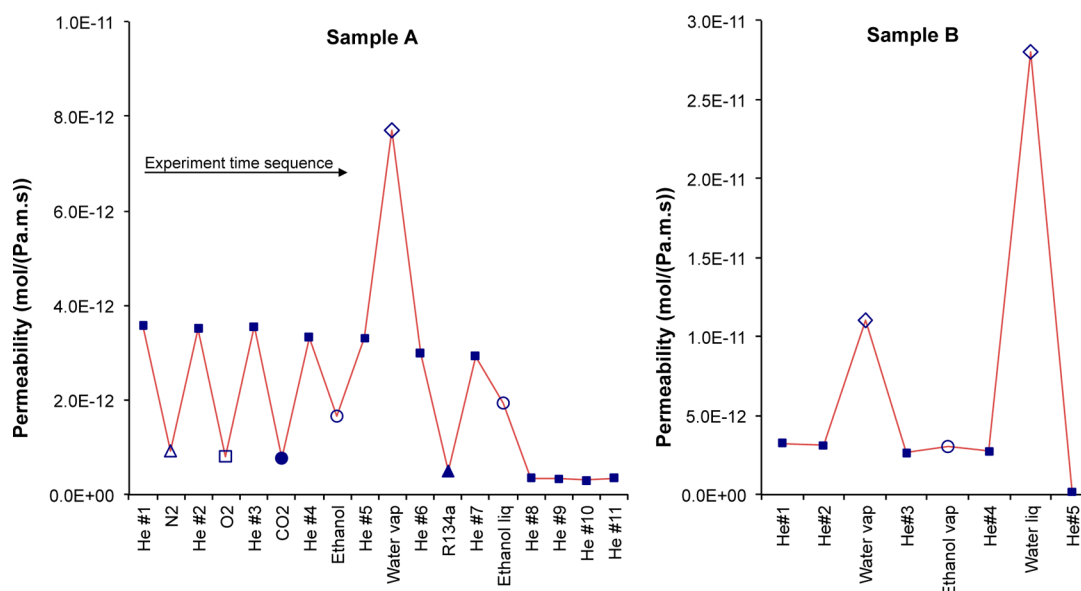


**Figure 2.** Permeabilities obtained for samples A and B presented in the experiment sequence. The permeability for He was approximately constant until the sample was exposed to liquid, water or ethanol. After liquid exposure, permeation to He was reduced.

**Table 2. Experimental Data from Permeability Tests<sup>a</sup>**

	sample A ( $10^{-13}$ mol/(m·s·Pa))		sample B ( $10^{-13}$ mol/(m·s·Pa))
He 1	35.6	He 1	32.4
N <sub>2</sub>	9.2	He 2	31.3
He 2	35.1	water vapor	110.1
O <sub>2</sub>	8.2	He 3	26.3
He 3	35.5	ethanol vapor	30.1
CO <sub>2</sub>	7.7	He 4	27.4
He 4	33.2	water liquid	280.5
ethanol vapor	16.6	He 5	1.9
He 5	33.1		
water vapor	77.0		
He 6	29.8		
R134a	5.0		
He 7	29.3		
ethanol liquid	19.2		
He 8	3.5		
He 9	3.3		
He 10	3.0		
He 11	3.5		

<sup>a</sup>Experiment sequence is from the first line to the last in both samples.

Several samples were tested, although we show the results of only two (identified as A and B). Testing more samples has a limited interest, because cork permeability shows a high (natural) variability. Even the permeability for water and ethanol vapors “normalized to He” showed considerable variability. Therefore, the results obtained with different permeant species should be compared within the same sample rather among samples.

Permeant species were selected to be N<sub>2</sub>, O<sub>2</sub>, CO<sub>2</sub>, H<sub>2</sub>O, and CH<sub>3</sub>CH<sub>2</sub>OH, mainly due to their possible relevance to wine. We also used He and C<sub>2</sub>H<sub>2</sub>F<sub>4</sub> (common refrigerant gas known as R134a) as light and heavy gases, respectively, because they are known to be inert. Because the permeability for He can be measured in a few minutes, it was used repeatedly to monitor any permanent change in the sample permeability after exposure to other permeants, particularly those in the liquid phase.

After tests with liquids, both samples were dried in an oven at 100 °C for at least 24 h, without disassembling them from the holder. After cooling, the final permeability for helium was tested.

The permeabilities of sample A were measured for the following species and sequence: helium, nitrogen, helium, oxygen, helium, carbon dioxide, helium, ethanol vapor, helium, water vapor, helium, liquid ethanol, and finally four consecutive tests with helium, one per day. The last tests were repeated because helium permeability had changed drastically after its exposure to liquid ethanol. Due to this change we did not expose sample A to water (liquid).

The permeabilities of sample B were evaluated for helium, ethanol vapor, helium, water vapor, helium, liquid water, and finally helium. Once again, after liquid exposure, the permeability for helium permanently changed. Therefore, this sample was not tested to liquid ethanol.

In the case of liquids, its vapor pressure was used as the pressure difference in eq 1 because higher pressures do not lead to any noticeable increased density of permeant in the feed side.

**Diffusion Measurements.** Diffusion coefficients from transient permeation can be calculated through the time-lag method, which considers valid the second Fick’s law for transient mass transport

through dense materials. The mass permeated through the membrane, directly related to the downstream pressure, is plotted over time, and the intercept of the line correspondent to the steady-state period with the  $x$ -axis is the time lag,  $\theta$ . The diffusion coefficient,  $D$ , can be calculated from the time lag,  $\theta$ , by the relationship

$$D = \frac{\delta^2}{6\theta} \quad (3)$$

where  $\delta$  is the sample thickness. If the time lag is very small, then diffusion is very fast, which may suggest that transport is performed by some alternative mechanism such as through pores or channels.

**Sorption Measurements.** Sorption was measured by thermogravimetry in two steps. In the first step, about 3 mg of cork was placed in a closed and sealed container with the headspace saturated of vapor during 1 week at a controlled temperature of  $23 \pm 2$  °C. Then, in the second step, desorption was followed by thermogravimetry. The saturated cork sample was introduced in a balance at 25 °C under a constant nitrogen flow of 20 mL/min, and its mass was recorded over time. The sorption coefficient can be calculated from the initial and final masses of the desorption step.

The sorption coefficient for each vapor  $i$  ( $i$  denotes the vapor species and becomes  $w$  for water and  $e$  for ethanol) given by

$$S_i = \frac{c_{i,\text{cork}}}{c_{i,\text{HS}}} \quad (4)$$

where  $c_{i,\text{cork}}$  is the concentration of vapor  $i$  (water or ethanol) in cork, in moles per gram of dry cork, and  $c_{i,\text{HS}}$  is the concentration in the container headspace, (during the sorption step), in moles per gram of dry air.

The concentration of vapor in cork  $c_{i,\text{cork}}$  is given by the relationship

$$c_{i,\text{cork}} = \frac{n_{i,s}}{m_d} \quad (5)$$

where  $n_{i,s}$  is the amount (in mol) of sorbed vapor and  $m_d$  the mass of dry cork. The concentration in the headspace is calculated from the vapor pressure  $p_{v,i}$  and the atmospheric pressure  $p_{\text{atm}}$  as follows:

$$c_{i,\text{HS}} = \frac{\frac{p_{v,i}}{p_{\text{atm}}}}{\left(1 - \frac{p_{v,i}}{p_{\text{atm}}}\right)} M_{\text{air}} \quad (6)$$

$M_{\text{air}}$  is the molecular weight of air in g/mol, at the temperature of the experiment.

## RESULTS

The results of permeability experiments performed with samples A and B are shown in Figure 2 and Table 2. For both samples, the results can be summarized as follows:

- In both samples the permeability for water and ethanol, in any phase, was higher than for any tested gas, except for the light gas helium. For example, the permeability for ethanol vapor was 2.2 times higher than for  $\text{CO}_2$ , despite similar molar masses.
- The permeability for water vapor was 4.6 and 3.6 times higher than the permeability for ethanol vapor, respectively, in samples A and B.
- The permeability for liquids was higher than the permeability for their vapors in both samples, 16 and 2.5% higher, respectively, for ethanol (sample A) and water (sample B).
- The permeability for helium remained approximately constant no matter the gases and vapors used in previous tests, which is an indication of no permanent change in the sample. On the contrary, the permeability for helium decreased drastically after the samples were exposed to

liquids: >8 times after exposure to liquid ethanol (sample A) and about 14 times after liquid water (sample B).

The diffusion coefficients of ethanol and water through cork were calculated from the time lag  $\theta$  (eq 3), which was obtained from the analysis of the downstream pressure plotted against time. Figures 3 and 4 show the pressure rise plots for water and

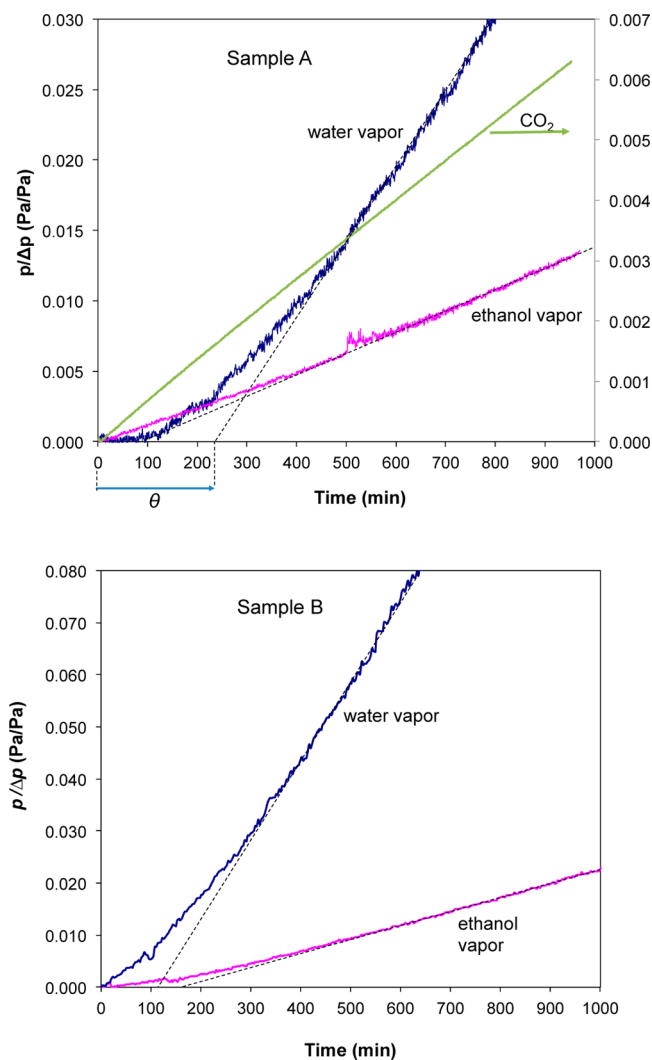


**Figure 3.** Downstream pressure (normalized to the pressure difference  $\Delta p = p_f - p_d$ ) for water and ethanol vapors. In sample A, the downstream pressure induced by the permeation of  $\text{CO}_2$  is also plotted.

ethanol. In Figure 3 the plot for  $\text{CO}_2$  is also presented. The permeation of water displays a peculiar behavior, starting at a very slow flow rate and then increasing until a steady-state permeation rate is achieved. Ethanol vapor also shows a similar development but reaching a lower flow rate. In the case of  $\text{CO}_2$ , the steady state is achieved almost immediately and the same happened for all other gases. The time lag was obtained from the intersection with the time axis of the tangent when a constant slope is reached (steady-state period), as presented in Figure 3.

The pressure evolution for liquid water showed similar behavior as for water vapor with a clear time lag needed to reach a constant slope. The time was about the same as for

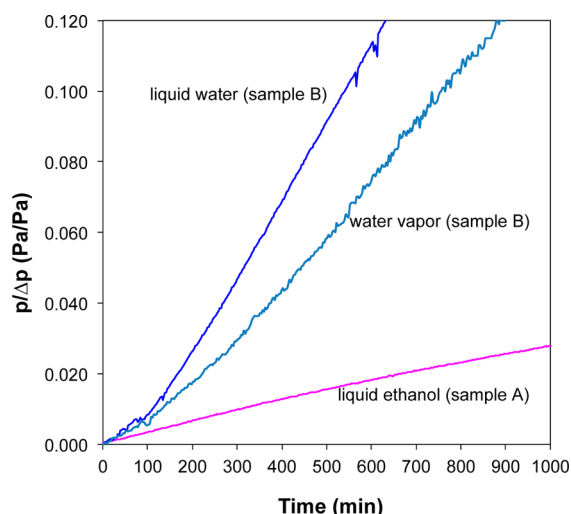


**Figure 4.** Downstream pressure (normalized to the pressure difference  $\Delta p$ ) for water (vapor and liquid) and liquid ethanol.

vapor in the same sample. In the case of liquid ethanol (sample A) the time lag was difficult to observe.

The diffusion coefficients of ethanol and water through cork calculated from the time lag (eq 3) are presented in Table 3 as

**Table 3.** Diffusion Coefficients Obtained in This Work and Comparison with Those Found in the Literature

permeant	diffusion coefficient ( $\text{m}^2 \cdot \text{s}^{-1}$ )	source
water vapor	$3.3 \times 10^{-11a}$ and $1.5 \times 10^{-10b}$	this work (time lag)
	$7.0 \times 10^{-12}$	ref 20
water, liquid	$1.4 \times 10^{-10b}$	this work (time lag)
	$(1.9\text{--}2.5) \times 10^{-11}$	ref 3
	$(0.28\text{--}1.2) \times 10^{-11}$	ref 18
ethanol vapor	$1.1 \times 10^{-10b}$	this work (time lag)

<sup>a</sup>Sample A. <sup>b</sup>Sample B.

are those found in the literature. As expected, for the same sample (sample A), the diffusion coefficients for ethanol vapor were lower than for water vapor, because ethanol is a larger molecule.

For the sorption experiment, Figure 5 shows the evolution of cork's mass during its exposure to ethanol and water vapors in the desorption step. Reaching a plateau corresponds to attaining equilibrium conditions. The mass of wet cork at the beginning of each desorption step,  $m_w$ , was taken at  $t = 0$ , and the mass of dry cork,  $m_d$ , is taken from the average between 9 and 12 h. The mass of water or ethanol sorbed by cork under equilibrium conditions,  $m_s$ , is the difference between  $m_w$  and  $m_d$ .

Calculated sorption coefficients are represented in Table 4. Results show that both ethanol and water have relevant affinity to cork, with water displaying more intense sorption. The highest sorption coefficient observed for water means that a certain amount of cork retains 3.5 times more water than the equivalent volume of saturated water vapor. To compare sorption coefficients for vapors and gases, Table 4 shows the sorption coefficient for He measured in a previous work<sup>10</sup> in ( $\text{mol}/\text{cm}^3_{\text{dry,cork}}/\text{Pa}$ ) units, also for water and ethanol.

The sorption coefficients of liquids were not measured due to the alveolar (not dense) structure of cork.

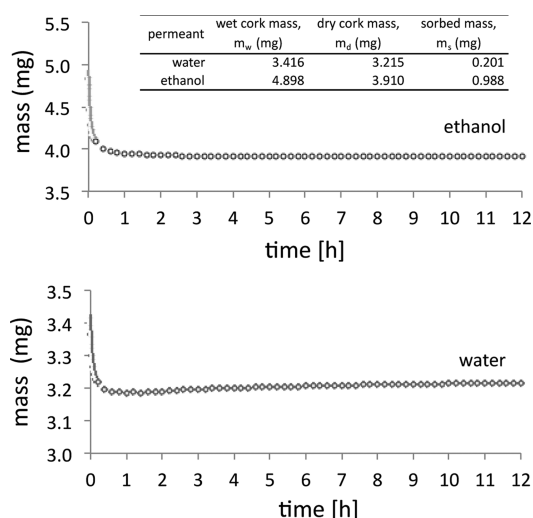


**Figure 5.** Desorption kinetics of water and ethanol vapors from cork. The mass of cork was recorded for 12 h after its saturation with vapor. Sample was at 25 °C under a constant nitrogen flow of 20 mL/min.  $m_w$  and  $m_d$  are respectively the mass of cork at the beginning and at the end of each desorption step, and  $m_s$  is the sorbed mass at equilibrium conditions.

**Table 4.** Sorption Coefficients of Water and Ethanol Vapors and of He in Boiled Cork at  $23 \pm 2$  °C

	sorption, S	
	(—)	( $\text{mol}/\text{cm}^3_{\text{cork}}/\text{Pa}$ )
water	3.5	$2.0 \times 10^{-7}$
ethanol	2.1	$1.3 \times 10^{-7}$
helium <sup>10</sup>	—	$1.1 \times 10^{-9}$

## DISCUSSION

Previous works have shown that gases permeate through cork via small conduits between cells, the plasmodesmata, following a Knudsen molecular flow behavior.<sup>9,10</sup> Calculations for the equivalent open diameter fitted quite well the ultrastructure observation of cork by transmission electron microscopy, leading to channel diameters in the range of 40–100 nm.

When we plot the permeability as a function of the permeant mass as in Figure 6, an important deviation is observed for vapors, with experimental permeability values higher than those estimated through a Knudsen molecular flow behavior. This deviation was more pronounced for liquid ethanol than for ethanol vapor. The permeability data of sample B (see Figure 2 and Table 2) show that water had a more pronounced deviation to Knudsen molecular flow behavior than ethanol.

1. In sample A, the permeability for water vapor deviated more from the model than in the case of ethanol vapor.
2. The liquid permeability was much higher than the vapor permeability in the case of water (sample B, 2.5 times higher). Similar behavior was also observed for ethanol, although less pronounced (sample A, 16% higher).
3. The permeability for helium after liquid permeation decreased more significantly in the case of liquid water permeation (sample B, 14 times lower) than in the case of liquid ethanol permeation (sample A, 8 times lower), showing a more drastic change in sample B (after liquid permeation).

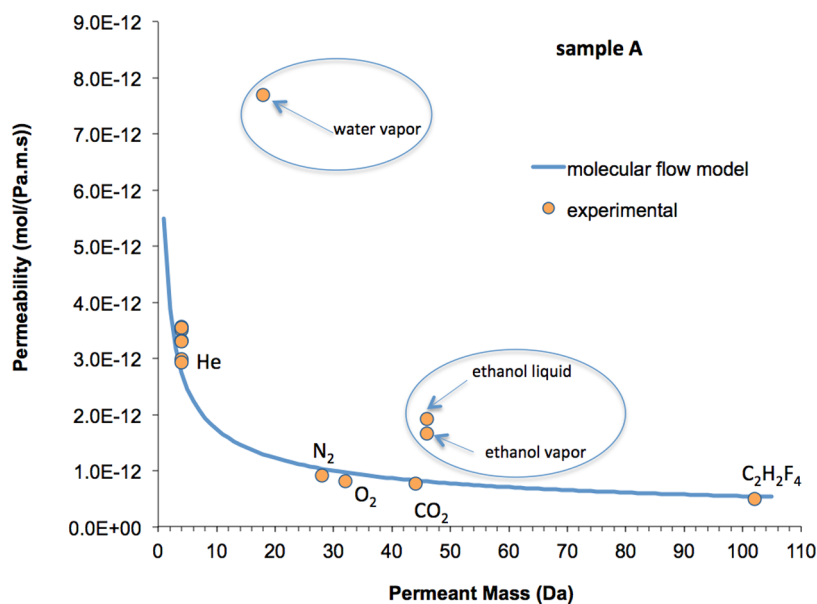


**Figure 6.** Permeability as a function of the permeant mass. Gas permeation through cork follows the model for Knudsen molecular gas flow in porous media, developed in refs 9 and 10, using different approaches. However, for water and ethanol vapors and for liquid ethanol this model is not adequate. Because the permeability is higher, an alternative transport mechanism is expected (Knudsen molecular flow behavior).

Therefore, the transport of ethanol and (especially) water in vapor and liquid phases through cork is not explained exclusively by a Knudsen molecular flow through plasmodesmata.

The sorption coefficients of water vapor and ethanol vapor in cork (see Table 4) were 2 orders of magnitude higher than the sorption coefficients of several gases obtained in ref 10 (the highest value obtained was  $2.4 \text{ cm}^3_{\text{gas}}(\text{STP})/\text{cm}^3_{\text{dry.cork}}/\text{atm}$  or  $1.1 \times 10^{-9} \text{ mol}_{\text{gas}}/\text{cm}^3_{\text{dry.cork}}/\text{Pa}$ ). Water and ethanol in the vapor phase exhibit much higher affinity to the cork cell walls than gases, for which cork cell walls perform as an inert material. These results suggest that part of the vapor and (also liquid) transport through cork is performed through the cork cell walls. Starting from this assumption, we believe the higher solubility of water vapor than ethanol vapor in cork is consistent with the stronger deviation of water transport to the Knudsen molecular flow model.

Diffusion coefficients calculated by time lag for water in vapor and liquid phases were analyzed. Diffusion coefficients calculated by time lag refer to mass transport through dense materials in the transient state, but the values obtained were always higher than the experimental values found in the literature. These results show that the transport of water (and also ethanol) in vapor and liquid phase is not exclusively explained by the sorption–diffusion model, typical for a dense material.

This work shows evidence that the transport of vapors through cork is partially explained by the transport through plasmodesmata channels and partially by the transport through the dense cork walls, unlike gas transport through cork. This alternative mechanism is illustrated in Figure 7.

This experimental observation was somewhat unexpected because cork is very often described as a watertight sealant. However, one should keep in mind that the highest stated permeability of  $280.5 \times 10^{-13} \text{ mol}/(\text{m}\cdot\text{s}\cdot\text{Pa})$  (for liquid water, see Figure 2 and Table 2) leads to  $<0.3 \text{ cm}^3$  of water loss through a standard cork closure after one year. Moreover, our experiments were performed with uncompressed cork.

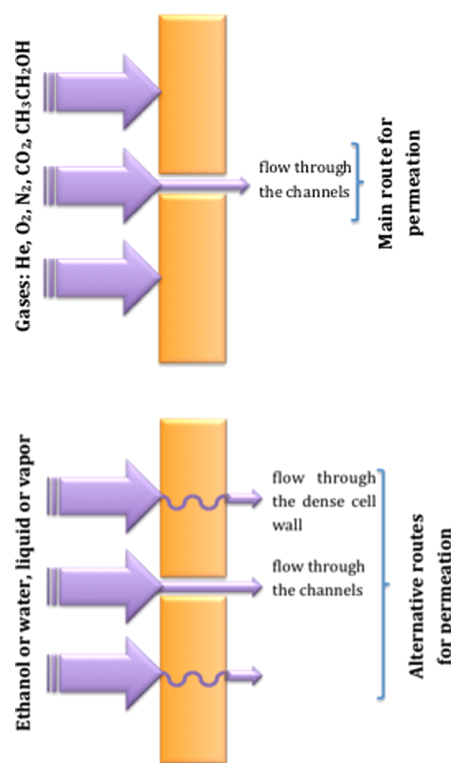


**Figure 7.** Proposed model for the transport of gases and vapors in cork. Contrarily to gases, vapors permeate not only by plasmodesmata but also through the dense wall of cork cell by sorption–diffusion, similarly to dense membranes.

The permeability for helium decreased by a factor of  $\approx 10$  after sample wetting by the selected liquids. Drying the sample in the oven at  $100 \text{ }^\circ\text{C}$  for longer than 24 h (without disassembling) did not reverse the change in permeability. This can be explained only by a change in cork.

In summary we may conclude the following:

- Water and ethanol permeate cork not only through the plasmodesmata but also through the cork cell walls. This is the case for both vapor and liquid phases.
- In our samples, wetting cork by water or ethanol changed permanently the permeation rate for gases.

These conclusions have implications in cork closures and their application in wine bottling. Stated permeabilities for oxygen<sup>25,28–33</sup> should be seen in the light of this work. Wet cork is expected to behave differently from dry cork with regard to gas permeation, as was the case of our samples. Once cork becomes soaked, oxygen ingress could be reduced by a factor of 10 as we measured for He in this work. It is also possible that the huge variability of permeation measured before for He (3 orders of magnitude) is significantly reduced for wet cork, in line with the results of other authors who tested cork closures under real conditions.<sup>28,34,35</sup> From this work it may be recommended that bottles should be placed horizontally for long-term storage of wine, assuring minimum oxygen ingress in the bottle, as is already common practice. As future work, the effect of a mixture of ethanol and water as well as wine will be used to assess the permeation and selectivity of cork to the main components of wine. Such research aims to understand more comprehensively the liquid and gas transport properties of natural cork under realistic conditions.

## AUTHOR INFORMATION

### Corresponding Author

\*(O.M.N.D.T.) Phone: +351 21 2948576. Fax: +351 21 2948549. E-mail: odt@fct.unl.pt.

### Funding

The financial support of the Portuguese Foundation for Science and Technology is gratefully acknowledged (PTDC/EME-MFE/098738/2008, PEst-OE/FIS/UI0068/2011, SFRH/BPD/45445/2008, and SFRH/BPD/79533/2011).

### Notes

The authors declare no competing financial interest.

## ACKNOWLEDGMENTS

We acknowledge Dr. Anabela Valente and Maria Celeste Azevedo of the CICECO, Departamento de Química, Universidade de Aveiro, for technical assistance with the thermogravimetry analysis and Nenad Bundaleski for the final English language revision.

## REFERENCES

- (1) Pereira, H. *Cork Biology Production and Uses*; Elsevier: Amsterdam, The Netherlands, 2007.
- (2) Silva, S. P.; Sabino, M. A.; Fernandes, E. M.; Correlo, V. M.; Boesel, L. F.; Reis, R. L. Cork: properties, capabilities and applications. *Int. Mater. Rev.* **2005**, *50*, 345–365.
- (3) Fortes, M. A.; Rosa, M. E.; Pereira, H. *A Cortiça*, 1st ed.; IST Press: Lisbon, Portugal, 2004; p 260.
- (4) Sousa, V. B.; Leal, S.; Quilhó, T.; Pereira, H. Characterization of cork oak (*Quercus suber*) wood anatomy. *IAWA J.* **2009**, *30*, 149–161.
- (5) Şen, A.; Miranda, I.; Santos, S.; Graça, J.; Pereira, H. The chemical composition of cork and phloem in the rhytidome of *Quercus cerris* bark. *Ind. Crops Prod.* **2010**, *31*, 417–422.
- (6) Pereira, H.; Rosa, M. E.; Fortes, M. A. The cellular structure of cork from *Quercus suber* L. *IAWA Bull.* **1987**, *8*, 213–218.
- (7) Pereira, H. Chemical composition and variability of cork from *Quercus suber* L. *Wood Sci. Technol.* **1988**, *22*, 211–218.
- (8) Teixeira, R. T.; Pereira, H. Suberized cell walls of cork from cork oak differ from other species. *Microsc. Microanal.* **2010**, *16*, 569–575.
- (9) Faria, D. P.; Fonseca, A. L.; Pereira, H.; Teodoro, O. M. N. D. Permeability of cork to gases. *J. Agric. Food Chem.* **2011**, *59*, 3590–3597.
- (10) Brazinha, C.; Fonseca, A. P.; Pereira, H.; Teodoro, O. M. N. D. Gas transport through cork: modelling gas permeation based on the morphology of a natural polymer material. *J. Membr. Sci.* **2013**, *428*, 52–62.
- (11) Teodoro, O. M. N. D.; Mesquita, A. C. Gas released from cork after bottling. *Bull. O. I. V.* **2011**, *84*, 361–369.
- (12) Villaescusa, I.; Martinez, M.; Miralles, N. Heavy metal uptake from aqueous solution by cork and yohimbe bark wastes. *J. Chem. Technol. Biotechnol.* **2000**, *75*, 812–816.
- (13) Machado, R.; Carvalho, J. R.; Correia, M. J. N. Removal of trivalent chromium(III) from solution by biosorption in cork powder. *J. Chem. Technol. Biotechnol.* **2002**, *77*, 1340–1348.
- (14) Chubar, N.; Carvalho, J. R.; Correia, M. J. N. Cork biomass as biosorbent for Cu(II), Zn(II) and Ni(II). *Colloids Surf. A* **2004**, *230*, 57–65.
- (15) Karbowiak, T.; Mansfield, A. K.; Barrera-García, V. D.; Chassagne, D. Sorption and diffusion properties of volatile phenols into cork. *Food Chem.* **2010**, *122*, 1089–1094.
- (16) Barker, D. A.; Capone, D. L.; Pollnitz, A. P.; McLean, H. J.; Francis, I. L.; Oakey, H.; Sefton, M. A. Absorption of 2,4,6-trichloroanisole by wine corks via the vapour phase in an enclosed environment. *Aust. J. Grape Wine Res.* **2001**, *7*, 40–46.
- (17) Capone, D. L.; Skouroumounis, G. K.; Sefton, M. A. Permeation of 2,4,6-trichloroanisole through cork closures in wine bottles. *Aust. J. Grape Wine Res.* **2002**, *8*, 196–199.
- (18) Lequin, S.; Chassagne, D.; Karbowiak, T.; Bellat, J.-P. Sorption equilibria of ethanol on cork. *J. Agric. Food Chem.* **2013**, *61*, 5391–5396.
- (19) Rosa, M. E.; Fortes, M. A. Water absorption by cork. *Wood Fiber Sci.* **1993**, *25*, 339–348.
- (20) Adão, H.; Veiga, I. M.; Fernandes, A. C.; Saramago, B. Water absorption by cellular polymers. *J. Mater. Sci. Lett.* **1996**, *15*, 1129–1131.
- (21) Lequin, S.; Chassagne, D.; Karbowiak, T.; Gougeon, R.; Brachais, L.; Bellat, J.-P. Adsorption equilibria of water vapor on cork. *J. Agric. Food Chem.* **2010**, *58*, 3438–3445.
- (22) Teti, A. J.; Rodriguez, D. E.; Federici, J. F.; Brisson, C. Non-destructive measurement of water diffusion in natural cork enclosures using terahertz spectroscopy and imaging. *J. Infrared Millimeter Waves* **2011**, *32*, 513–527.
- (23) Rosa, M. E.; Fortes, M. A. Recovery of used cork stoppers. *Colloids Surf. A* **2009**, *344*, 97–100.
- (24) Mas, A.; Puig, J.; Llado, N.; Zamora, F. Sealing and storage position effects on wine evolution. *J. Food Sci.* **2002**, *67*, 1374–1378.
- (25) Lopes, P.; Saucier, C.; Teissedre, P.-L.; Glories, Y. Impact of storage position on oxygen ingress through different closures into wine bottles. *J. Agric. Food Chem.* **2006**, *54*, 6741–6746.
- (26) Skouroumounis, G. K.; Kwiatkowski, M. J.; Francis, I. L.; Oakey, H.; Capone, D. L.; Duncan, B.; Sefton, M. A.; Waters, E. J. The impact of closure type and storage conditions on the composition, colour and flavour properties of a Riesling and a wooded Chardonnay wine during five years' storage. *Aust. J. Grape Wine Res.* **2005**, *11*, 369–383.
- (27) Rutherford, S. W.; Do, D. D. Review of time lag permeation technique as a method for characterisation of porous media and membranes. *Adsorption* **1997**, *3*, 283–312.
- (28) Lopes, P.; Ceadric, S.; Glories, Y. Nondestructive colorimetric method to determine the oxygen diffusion rate through closures used in winemaking. *J. Agric. Food Chem.* **2005**, *53*, 6967–6973.
- (29) Godden, P.; Lattey, K.; Francis, L.; Gishen, M.; Cowey, G.; Robinson, E.; Waters, E.; Skouroumounis, G.; Sefton, M. Towards offering wine to the consumer in optimal condition – the wine, the closures and other packaging variables: a review of AWRI research examining the changes that occur in wine after bottling. *Aust. N. Z. Wine Ind. J.* **2005**, *20*, 20–30.

(30) Hart, A.; Kleinig, A. *The Role of Oxygen in the Aging of Bottled Wine*; Wine Press Club of New South Wales Australia: Sydney, Australia, 2005; pp 1–14.

(31) Karbowiak, T.; Gougeon, R. D.; Alinc, J.-B.; Brachais, L.; Debeaufort, F.; Voilley, A.; David, C. Wine oxidation and the role of cork. *Crit. Rev. Food Sci. Nutr.* **2010**, *50*, 20–52.

(32) Lequin, S.; Chassagne, D.; Karbowiak, T.; Simon, J.-M.; Paulin, C.; Bellat, J.-P. Diffusion of oxygen in cork. *J. Agric. Food Chem.* **2012**, *60*, 3348–3356.

(33) Silvia, M. A.; Julien, M.; Jourdes, M.; Teissedre, P.-L. Impact of closures on wine post-bottling development: a review. *Eur. Food Res. Technol.* **2011**, *233*, 905–914.

(34) Brotto, L.; Battistutta, F.; Tat, L.; Comuzzo, P.; Zironi, R. Modified nondestructive colorimetric method to evaluate the variability of oxygen diffusion rate through wine bottle closures. *J. Agric. Food Chem.* **2010**, *58*, 3567–3572.

(35) González-Adrados, J. R.; González-Hernández, F.; de Ceca, J. L. G.; Cáceres-Esteban, M. J.; García-Vallejo, M. C. Wine absorption by cork stoppers. *Span. J. Agric. Res.* **2008**, *6*, 645–649.